JCI The Journal of Clinical Investigation

STRADα deficiency results in aberrant mTORC1 signaling during corticogenesis in humans and mice

Ksenia A. Orlova, … , Kevin Strauss, Peter B. Crino

J Clin Invest. 2010;120(5):1591-1602. https://doi.org/10.1172/JCI41592.

Research Article

Polyhydramnios, megalencephaly, and symptomatic epilepsy syndrome (PMSE) is a rare human autosomal-recessive disorder characterized by abnormal brain development, cognitive disability, and intractable epilepsy. It is caused by homozygous deletions of STE20-related kinase adaptor α (*STRADA*). The underlying pathogenic mechanisms of PMSE and the role of *STRADA* in cortical development remain unknown. Here, we found that a human PMSE brain exhibits cytomegaly, neuronal heterotopia, and aberrant activation of mammalian target of rapamycin complex 1 (mTORC1) signaling. STRADα normally binds and exports the protein kinase LKB1 out of the nucleus, leading to suppression of the mTORC1 pathway. We found that neurons in human PMSE cortex exhibited abnormal nuclear localization of LKB1. To investigate this further, we modeled PMSE in mouse neural progenitor cells (mNPCs) in vitro and in developing mouse cortex in vivo by knocking down STRADα expression. STRADα-deficient mNPCs were cytomegalic and showed aberrant rapamycin-dependent activation of mTORC1 in association with abnormal nuclear localization of LKB1. Consistent with the observations in human PMSE brain, knockdown of STRADα in vivo resulted in cortical malformation, enhanced mTORC1 activation, and abnormal nuclear localization of LKB1. Thus, we suggest that the aberrant nuclear accumulation of LKB1 caused by STRADα deficiency contributes to hyperactivation of mTORC1 signaling and disruption of neuronal lamination during corticogenesis, and thereby the neurological features associated with PMSE.

STRADα deficiency results in aberrant mTORC1 signaling during corticogenesis in humans and mice

Ksenia A. Orlova,[1] Whitney E. Parker,[1] Gregory G. Heuer,[2] Victoria Tsai,[1] Jason Yoon,[3] Marianna Baybis,[1] Robert S. Fenning,[4] Kevin Strauss,[5] and Peter B. Crino[1]

[1]Penn Epilepsy Center and Department of Neurology, [2]Department of Neurosurgery, [3]Department of Arts and Sciences, and [4]Department of Medicine, University of Pennsylvania Medical Center, Philadelphia, Pennsylvania, USA. [5]The Clinic for Special Children, Lancaster, Pennsylvania, USA.

Polyhydramnios, megalencephaly, and symptomatic epilepsy syndrome (PMSE) is a rare human autosomal-recessive disorder characterized by abnormal brain development, cognitive disability, and intractable epilepsy. It is caused by homozygous deletions of STE20-related kinase adaptor α (*STRADA*). The underlying pathogenic mechanisms of PMSE and the role of *STRADA* in cortical development remain unknown. Here, we found that a human PMSE brain exhibits cytomegaly, neuronal heterotopia, and aberrant activation of mammalian target of rapamycin complex 1 (mTORC1) signaling. STRADα normally binds and exports the protein kinase LKB1 out of the nucleus, leading to suppression of the mTORC1 pathway. We found that neurons in human PMSE cortex exhibited abnormal nuclear localization of LKB1. To investigate this further, we modeled PMSE in mouse neural progenitor cells (mNPCs) in vitro and in developing mouse cortex in vivo by knocking down STRADα expression. STRADα-deficient mNPCs were cytomegalic and showed aberrant rapamycin-dependent activation of mTORC1 in association with abnormal nuclear localization of LKB1. Consistent with the observations in human PMSE brain, knockdown of STRADα in vivo resulted in cortical malformation, enhanced mTORC1 activation, and abnormal nuclear localization of LKB1. Thus, we suggest that the aberrant nuclear accumulation of LKB1 caused by STRADα deficiency contributes to hyperactivation of mTORC1 signaling and disruption of neuronal lamination during corticogenesis, and thereby the neurological features associated with PMSE.

Introduction

Rare disorders of central nervous system development can provide novel insights into normal brain formation during embryogenesis. Polyhydramnios, megalencephaly, and symptomatic epilepsy syndrome (PMSE; colloquially referred to as pretzel syndrome) is a newly described autosomal-recessive neurodevelopmental disorder that was identified in the Old Order Mennonite pediatric population of Lancaster, Pennsylvania, USA (1). PMSE is characterized by macrocephaly, craniofacial dysmorphism, hypotonia, severe cognitive disability, and medically intractable epilepsy. Single nucleotide polymorphism autozygosity mapping identified a large truncating C-terminal homozygous deletion in STE20-related kinase adaptor α (*STRADA*; also known as *LYK5*) in all affected children (1). Heterozygous parents are phenotypically normal, and expressing the truncated PMSE STRADα mutant (residues 1–251) in heterologous cell lines yields minimal protein levels, which suggests that the genomic deletion in *STRADA* confers a loss-of-function phenotype (2). To our knowledge, mutations in *STRADA* have not been previously linked to a human disorder, and little is known about the role of STRADα in the neuropathogenesis of PMSE or in normal cortical development.

STRADα functions as a pseudokinase that consists of a STE20-like kinase domain but lacks several residues indispensable for intrinsic catalysis (2, 3). It binds to and regulates the subcellular localization and activity of Ser/Thr kinase 11 (STK11; also known as LKB1; refs. 3–6). STRADα binding results in nuclear export of LKB1 and significantly augments the catalytic activity of LKB1 toward downstream substrates (2–6). LKB1 modulates cell growth, proliferation, polarization, apoptosis, and migration and acts as a master activating kinase to AMPK-related kinases (7–10). LKB1 and STRADα form a heterotrimeric complex with the small scaffolding protein MO25 (11), which helps to stabilize the LKB1-STRADα interaction (2, 5, 6, 11).

LKB1 regulates the mammalian target of rapamycin (mTOR) through the AMPK–tuberous sclerosis complex 2:tuberous sclerosis complex 1 (AMPK-TSC2:TSC1) pathway (refs. 12, 13, and Supplemental Figure 1; supplemental material available online with this article; doi:10.1172/JCI41592DS1). AMPK is an energy sensor activated by an increasing AMP/ATP ratio; this activation leads to a conformational change that permits phosphorylation of Thr172 on its activation loop by LKB1 (8). AMPK phosphorylates TSC2, activating the TSC2:TSC1 complex to suppress mTOR signaling (14, 15). mTOR is a 280-kDa Ser/Thr kinase that binds to raptor or rictor to form mTOR complex 1 (mTORC1) or mTORC2, respectively. mTORC1 is sensitive to the macrolide antibiotic rapamycin and regulates a myriad of processes, including translation, transcription, ribosome biogenesis, cell growth, autophagy, and metabolism (16). Mutations in *LKB1* cause Peutz-Jeghers syndrome (PJS), an autosomal-dominant disorder characterized by intestinal polyposis, mucocutaneous pigmentation, and increased cancer incidence (17). Gastrointestinal polyps from PJS patients and heterozygous *Lkb1*$^{+/-}$ mice exhibit evidence of mTORC1 hyperactivation (18–20).

Conflict of interest: The authors have declared that no conflict of interest exists.
Citation for this article: *J Clin Invest.* 2010;120(5):1591–1602. doi:10.1172/JCI41592.

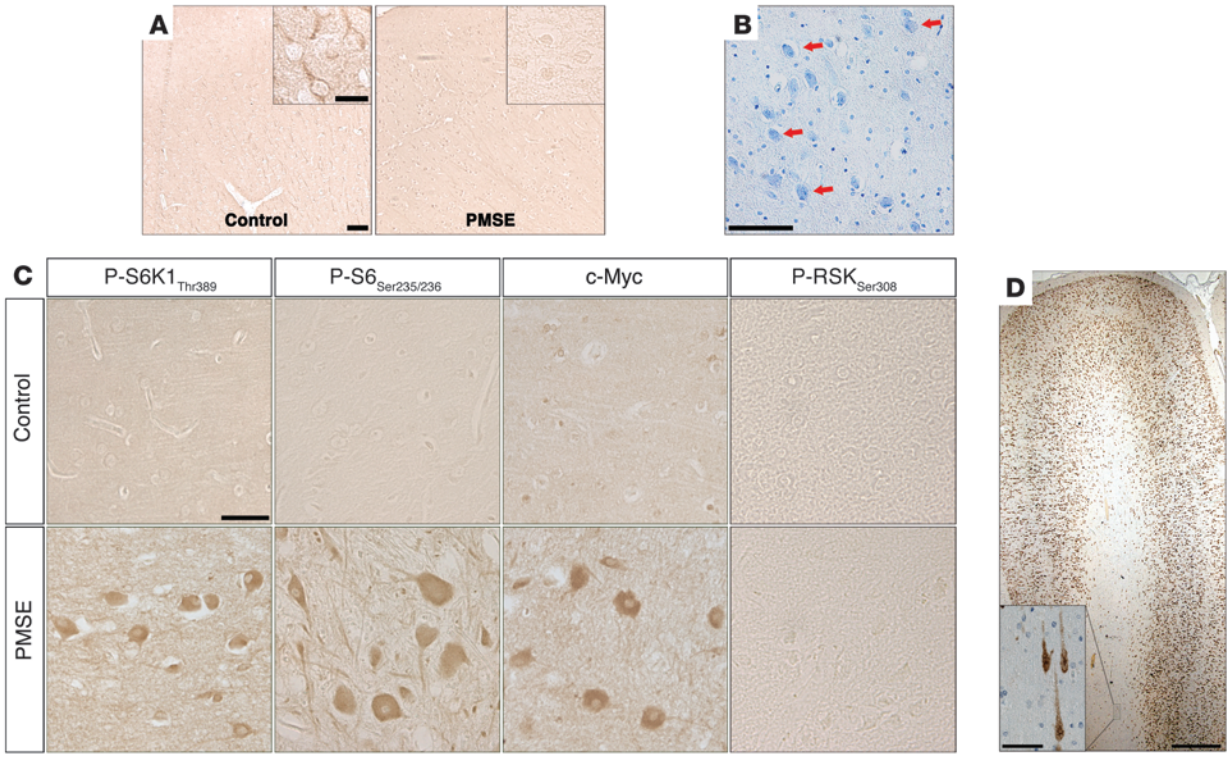

Figure 1
PMSE cortex exhibits cytomegaly, mTORC1 pathway activation, and neuronal heterotopia in the subcortical white matter. (**A**) Immunohistochemical analysis of control and PMSE cortex for STRADα demonstrated robust STRADα immunoreactivity in control, but not PMSE, cortex. (**B**) LFB-CV–stained section from the basal ganglia of a patient with PMSE, demonstrating numerous cytomegalic cells (arrows). (**C**) Immunohistochemistry of control and PMSE brain tissue for P-S6K1$_{Thr389}$, P-S6$_{Ser235/236}$, c-Myc, and P-RSK$_{Ser308}$, suggestive of mTORC1 cascade hyperactivation in PMSE brain. (**D**) Immunohistochemistry for NeuN of LFB-CV–stained cortical section from a PMSE patient demonstrating numerous NeuN$^+$ neurons in the subcortical white matter. Inset shows higher-magnification view of the boxed region. Scale bars: 100 μm (**A**), 20 μm (**A**, inset); 50 μm (**B**, **C**, and **D**, inset); 1 mm (**D**).

Several neurodevelopmental disorders result from mutations in genes that normally inhibit mTORC1 signaling. For example, *TSC1* or *TSC2* mutations result in tuberous sclerosis complex (TSC), characterized by cortical tubers, epilepsy, and cognitive disability, whereas mutations in *PTEN*, which normally inhibits mTORC1 by antagonizing PI3K-PDK1-Akt signaling (21), have been reported in patients with autism and macrocephaly (22, 23). Hyperactivation of mTORC1 may therefore provide a common pathogenic mechanism for neurological disorders associated with altered brain structure, epilepsy, autism, and cognitive dysfunction.

The identification of PMSE provides a unique opportunity to investigate STRADα as a protein that may play an important role in cortical development. We show here that PMSE brain tissue exhibited aberrant mTORC1 activation and neuronal heterotopia. Knockdown of STRADα in mouse neural progenitor cells (mNPCs) caused enhanced mTORC1 signaling and cytomegaly that was prevented by rapamycin treatment. Depletion of STRADα during corticogenesis in vivo led to abnormal accumulation of cells in the proliferative zones of the embryonic brain in association with mTORC1 hyperactivity. We propose that STRADα deficiency leads to aberrant mTORC1 signaling in part by precluding nuclear export of LKB1, and our findings showed abnormal nuclear LKB1 localization in PMSE brain tissue and STRADα-deficient mNPCs. Our results indicate that STRADα plays a critical role during cortical development in part by modulating LKB1-dependent inhibition of mTORC1 signaling and suggest a mechanism by which STRADα loss leads to the neurological manifestations of PMSE.

Results

PMSE brain exhibits cytomegaly, heterotopia, and mTORC1 activation. An Ab recognizing an internal region of STRADα was used to probe control and PMSE cortex (Figure 1A). Neurons and astrocytes in all layers of control cortex exhibited abundant STRADα expression, whereas PMSE cortex was devoid of STRADα immunoreactivity. The phosphorylation state of mTORC1 targets S6 and S6K1 is often used to assess mTORC1 activity. In the original paper defining PMSE, clusters of cytomegalic neurons that exhibited S6 hyperphosphorylation were observed (1). More comprehensive investigation revealed additional evidence of mTORC1 hyperactivation in PMSE: enlarged cells exhibiting hyperphosphorylation of S6$_{Ser235/236}$ were noted in the basal ganglia, thalamus, and pons of PMSE, but not control, brain specimens (Figure 1, B and C). S6 is phosphorylated on Ser235/236 in an mTORC1-dependent manner by S6 kinase 1 (S6K1; ref. 16) as well as via Ras/ERK signaling by ribosomal S6 kinase (RSK; ref. 24). To distinguish between these pathways, the phosphorylation status of S6K1$_{Thr389}$ and RSK$_{Ser308}$ was assessed in PMSE and control brain sections. Enhanced

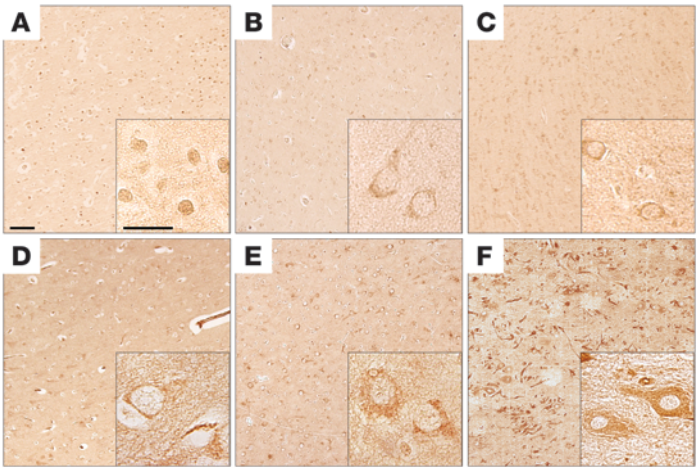

Figure 2
Cortical neurons in PMSE brain exhibit exclusively nuclear LKB1. Immunostaining for LKB1 in cortical specimens from PMSE (**A**), nonepilepsy control (**B**), cortical dysplasia focal epilepsy syndrome (**C**), sporadic type II focal cortical dysplasia (**D**), hemimegalencephaly (**E**), and TSC (**F**) cortical sections. Nearly all neurons in PMSE cortex (95%) exhibited exclusively nuclear LKB1 staining, unlike nonepilepsy control (5%). The majority of neurons in all other specimens showed predominately cytoplasmic LKB1 localization. Scale bars: 100 μm; 25 μm (insets).

P-S6K1$_{Thr389}$ immunoreactivity was identified in PMSE, but not control, brain (Figure 1C), whereas P-RSK$_{Ser308}$ immunoreactivity was minimal in both PMSE and control tissue, which suggests that loss of STRADα leads specifically to S6K1-mediated phosphorylation of S6. mTORC1 regulates translation of c-Myc through a 4E-BP1–dependent mechanism (25). Robust c-Myc expression was observed in PMSE, but not control, brain specimens (Figure 1C), supporting STRADα-mediated mTORC1 activation. To further define PMSE-associated neuropathology, brain sections stained with luxol fast blue–cresyl violet (LFB-CV) were probed for the neuron-specific antigen NeuN. Numerous NeuN$^+$ heterotopic neurons were found in the subcortical white matter in association with blurring of the gray-white matter junction (Figure 1D). These findings are highly suggestive of a neuronal migratory defect during cortical development.

Neurons in PMSE cortex exhibit exclusively nuclear LKB1 localization. One of the principal functions of STRADα is to shuttle LKB1 from the nucleus to the cytoplasm (3–5). Since PMSE results from loss of STRADα, we hypothesized that nucleocytoplasmic transport of LKB1 would be impaired in PMSE. We evaluated the subcellular localization of LKB1 by immunohistochemistry in PMSE cortex compared with control brain. The overwhelming majority (i.e., 95%) of cortical PMSE neurons exhibited exclusively nuclear LKB1, whereas in control brain, LKB1 was observed largely in the cytoplasm, and 5% of cells contained more nuclear than cytoplasmic LKB1 (Figure 2, A and B). These data corroborate previous reports that STRADα is essential for nuclear export of LKB1 and provide a possible mechanism for STRADα-mediated hyperactivation of mTORC1 signaling. We further investigated the subcellular localization of LKB1 in another neurodevelopmental disorder found in the Amish population, cortical dysplasia focal epilepsy syndrome (26), and in other, more common, brain malformations, such as sporadic type II focal cortical dysplasia, hemimegalencephaly, and TSC (Figure 2, C–F). In contrast to nuclear LKB1 in PMSE, LKB1 localization was predominately cytoplasmic in all these specimens. These findings were confirmed using 2 additional commercially available anti-LKB1 Abs (Supplemental Figure 2).

STRADα is expressed throughout the mouse brain at E17.0. To determine whether STRADα is expressed during normal murine corticogenesis, we immunostained brains of E17.0 C57BL/6 mice for STRADα. Sections were counterstained with Hoechst to visualize cell nuclei and identify the zones of the developing mouse cortex (Figure 3, A and D). STRADα was broadly expressed throughout the embryonic mouse brain by nestin$^+$ radial glia progenitor cells in the ventricular zone/subventricular zone (VZ/SVZ; Figure 3, B and C) and microtubule-associated protein–2–positive (MAP2$^+$) postmitotic neurons in the cortical plate (CP; Figure 3, E and F). STRADα expression was also present in the intermediate zone (IZ). These findings corroborate a previous report of *Strada* mRNA expression in the embryonic mouse brain at E15 (27). The developmental cortical expression profile of STRADα parallels LKB1 expression in neuronal cells during different stages of differentiation throughout the various zones of the embryonic mouse brain (27).

Depletion of STRADα in mNPCs in vitro. Since the histopathological features of PMSE reflect a neurodevelopmental abnormality, we next sought to model STRADα deficiency in vitro using both transient and stable knockdown approaches in mNPCs. These cells have been fully characterized previously (28, 29) and express sex determining region Y–box 2 (SOX2) and nestin (Supplemental Figure 3). STRADα was depleted transiently in mNPCs by transfection with 3 different GFP-tagged shRNA sequences (GFP-shRNA) that targeted disparate regions of endogenous *Strada* mRNA (Figure 4, A–G). In a parallel set of experiments, mNPCs were transfected with a GFP-shRNA containing a scrambled sequence that does not recognize any known mouse mRNA (GFP-shRNA scram) as a control. At 5 days post transfection (DPT), mNPCs were FACS sorted, and the enriched GFP$^+$ cell population was analyzed by immunoblotting for STRADα (Figure 4A). GFP-shRNA STRADα clone 3 resulted in efficient and reproducible STRADα knockdown and was used in all subsequent knockdown experiments (referred to hereafter as GFP-shRNA STRADα). Successful STRADα knockdown was confirmed by immunocytochemistry (Figure 4, B–G). We also established a stable STRADα-deficient mNPC line by transfection of mNPCs with a plasmid coexpressing a puromycin-resistant gene with an shRNA targeting *STRADA* (puro-shRNA STRADα; Figure 4H). In a parallel set of experiments, mNPCs were transfected with puro-shRNA scram. STRADα expression was reduced in puro-shRNA STRADα–transfected lines compared with puro-shRNA scram–transfected and untransfected wild-type mNPCs as assessed by immunoblotting (Figure 4H).

Knockdown of STRADα in mNPCs results in mTORC1 hyperactivity. LKB1 inhibits mTORC1 signaling by activating AMPK during periods of cellular stress (12–14). 5-Aminoimidazole-4-carboxamide-1-b-riboside (AICAR) is an AMPK agonist that simulates the effects of increasing AMP/ATP ratio by its intracellular conversion to AICAR monophosphate (ZMP; Supplemental Figure 1 and ref. 30). We first sought to confirm that functional LKB1 is required for suppression of mTORC1 signaling in response to AICAR treatment in mouse embryonic fibroblasts (MEFs). AICAR treatment of wild-type MEFs leads to AMPK activation and subsequent mTORC1

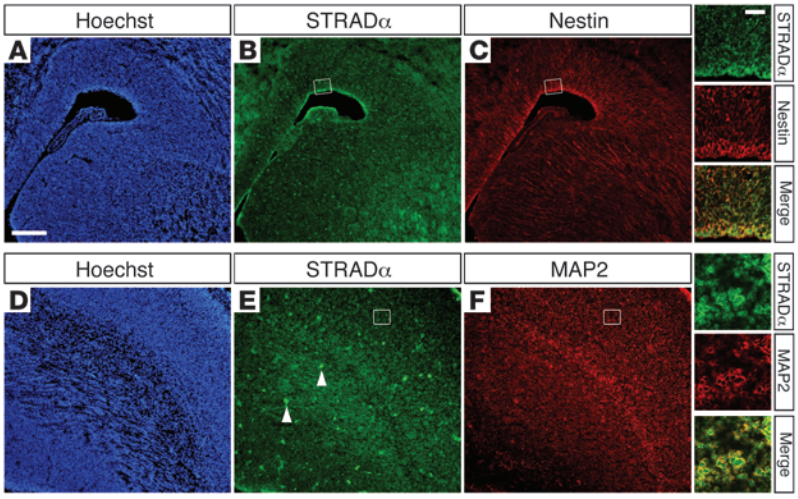

Figure 3
STRADα is expressed by nestin+ neural progenitor cells in the VZ/SVZ and by MAP2+ neurons in the CP at E17.0. Nuclei were visualized with Hoechst staining (**A** and **D**). Images at right are higher-magnification confocal views of boxed regions in **B**, **C**, **E**, and **F**. (**A**–**C**) Coimmunostaining for nestin (**C**) and STRADα (**B**) demonstrated STRADα expression in nestin+ radial glial neural progenitors in the VZ/SVZ (yellow in merged image). (**D**–**F**) Coimmunostaining for MAP2 (**F**) and STRADα (**E**) demonstrated expression of STRADα by MAP2+ neurons in the CP (yellow in merged image). Arrowheads in **E** delineate several blood vessels. Scale bar: 100 μm; 24 μm (higher-magnification views).

inhibition (13). In contrast, addition of AICAR to LKB1-null MEFs fails to activate AMPK and results in hyperactivation of mTORC1 signaling (refs. 8, 13 and Supplemental Figure 4).

Since the primary function of STRADα is to mediate LKB1 localization and activation (2, 3), we hypothesized that STRADα knockdown leads to hyperactivated mTORC1 signaling. To test this hypothesis, 5-DPT GFP-shRNA STRADα–transfected mNPCs were serum starved for 12 hours in the absence or presence of 2 mM AICAR and immunostained for P-S6$_{Ser235/236}$ (Figure 5, A–L). Untransfected and GFP-shRNA scram–transfected mNPCs decrease P-S6 levels after AICAR treatment (Figure 5, G–I) compared with vehicle-treated cells (Figure 4, A–C). STRADα-depleted mNPCs, however, failed to attenuate P-S6 levels in response to AICAR treatment (Figure 5, D–F and J–L). These findings were corroborated using STRADα-deficient mNPC lines (Figure 5M). Wild-type mNPCs as well as mNPCs stably transfected with puro-shRNA scram or puro-shRNA STRADα were serum starved overnight in the presence or absence of 2 mM AICAR. Additionally, cells were treated with 50 nM rapamycin for 1.5 hours. Protein lysates were assayed by immunoblotting for P-S6$_{Ser235/236}$ and total S6. Wild-type and puro-shRNA scram–transfected mNPCs exhibited decreased P-S6 levels following treatment with AICAR, rapamycin, or AICAR with rapamycin. STRADα-depleted mNPCs, however, failed to attenuate P-S6 after AICAR treatment. Addition of rapamycin following AICAR treatment diminished S6 phosphorylation, confirming that hyperphosphorylation of S6 in STRADα-depleted mNPCs resulted from mTORC1 signaling. Thus, STRADα knockdown failed to inhibit AICAR-mediated mTORC1 signaling in a rapamycin-dependent manner. These results support the hypothesis that STRADα deficiency in mNPCs leads to mTORC1 activation and suggest that STRADα functions as a novel mTORC1 regulatory protein in neural progenitor cells.

To investigate the ability of PMSE cells to attenuate P-S6 levels following energy depletion, we established lymphoblastoid cell lines (LCLs) from peripheral blood of PMSE patients, heterozygous parents, and controls (Supplemental Figure 4). Because AICAR has been previously shown to not activate AMPK in lymphocytes (31) and did not decrease P-S6 levels in control LCLs, we treated these cells with another known activator of AMPK, oligomycin (14). Cells were also pretreated with the Ca^{2+}/calmodulin-dependent protein kinase kinase inhibitor STO-609 (32) in order to evaluate the individual contribution of LKB1-mediated AMPK activation to inhibition of mTORC1 signaling. Oligomycin-treated PMSE LCLs failed to attenuate P-S6 levels, in contrast to control and heterozygous LCLs. These results lend further support to our hypothesis that STRADα deficiency results in mTORC1 hyperactivation and provide examples of aberrant mTORC1 signaling in non-neuronal cells from PMSE patients.

STRADα regulates cell size in a rapamycin-dependent manner. Cytomegaly is a hallmark of mTORC1 hyperactivity (33). To test the hypothesis that the observed cytomegaly in PMSE cortex is linked to STRADα deficiency via mTORC1 signaling, mNPCs were transfected with either GFP-shRNA STRADα or GFP-shRNA scram plasmids, and the cell area of untransfected wild-type mNPCs, GFP-shRNA scram–transfected cells, and GFP-shRNA STRADα–transfected cells was assessed at 10 DPT (n = 30 per group). The mean cell area of STRADα-depleted mNPCs (1,428 μm^2) was nearly twice that of wild-type and GFP-shRNA scram–transfected cells (719 and 722 μm^2, respectively; $P < 0.01$, both comparisons; Figure 6, A, C, and E). When cultured in the presence of daily rapamycin application, STRADα-depleted cells were similar in size (714 μm^2) to wild-type and GFP-shRNA scram–transfected mNPCs (694 and 672 μm^2, respectively; Figure 6, B, D, and E). Rapamycin application had no significant effect on the size of wild-type or GFP-shRNA scram–transfected mNPCs. Thus, STRADα depletion causes cytomegaly of mNPCs, which is prevented by rapamycin treatment.

STRADα-depleted mNPCs exhibit nuclear LKB1 localization. STRADα has been demonstrated to be critical for nuclear export of LKB1 in heterologous cell lines (4). Because analysis of PMSE brain tissue revealed exclusively nuclear LKB1, we evaluated the subcellular localization of endogenous LKB1 in wild-type, puro-shRNA scram–transfected, and puro-shRNA STRADα–transfected mNPCs. To ensure the specificity of the anti-LKB1 Ab, several Abs were first tested by immunocytochemistry of wild-type and LKB1-null MEFs (data not shown). Wild-type and puro-shRNA scram–transfected cells demonstrated predominately cytoplasmic LKB1 expression (Figure 7, A–D). STRADα-depleted cells, however, exhibited 69% and 73% more nuclear LKB1 immunoreactivity than did wild-type and puro-shRNA scram–transfected mNPCs, respectively ($P < 0.01$, both comparisons; Figure 7, E–G). These observations indicate that knockdown of endogenous STRADα in mNPCs results in nuclear accumulation of endogenous LKB1, supporting our findings in PMSE brain.

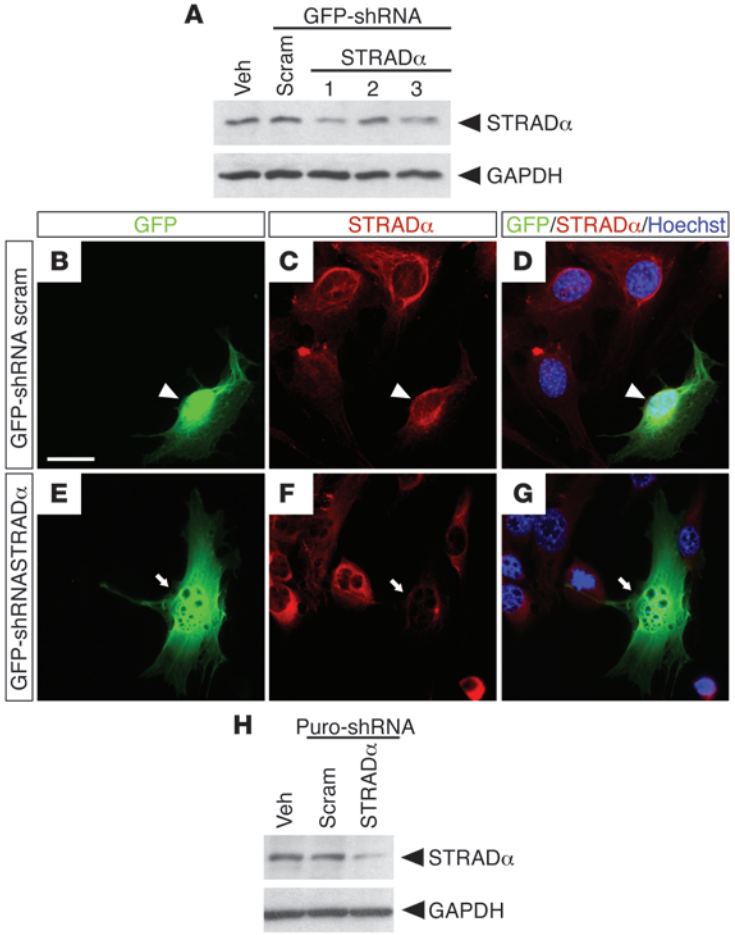

Figure 4
STRADα knockdown in mNPCs. (**A**–**G**) Transient knockdown of STRADα in mNPCs using GFP-shRNA. (**A**) mNPCs were transfected with vehicle (veh), GFP-shRNA scram, or GFP-shRNA STRADα clones 1–3 and FACS sorted for GFP expression at 5 DPT. Endogenous STRADα expression was assessed by immunoblotting. The blot was reprobed for GAPDH to assess equal loading. Cells were transfected, sorted, and immunoblotted in 3 separate experiments. GFP-shRNA STRADα clone 3 resulted in reproducible knockdown of STRADα. (**B**–**G**) mNPCs were transfected with GFP-shRNA STRADα clone 3 (**E**–**G**) or control GFP-shRNA scram (**B**–**D**) and immunostained for STRADα at 5 DPT. Nuclei were visualized with Hoechst staining (blue, **D** and **G**). A GFP-shRNA STRADα clone 3–transfected cell (arrows, **E**–**G**) exhibited less immunoreactivity for STRADα than did a GFP-shRNA scram–transfected cell (arrowhead, **B**–**D**) or untransfected neighboring cells. (**H**) Stable knockdown of STRADα using puro-shRNA. mNPCs were transfected with puro-shRNA scram or puro-shRNA STRADα, and transfected cells were selected for in the presence of puromycin. Expression of endogenous STRADα was assessed by immunoblotting approximately 6 weeks post transfection. Untransfected wild-type mNPCs (veh) were used as a control. The blot was reprobed for GAPDH to assess equal loading. Data are representative of 3 separate experiments. Scale bar: 20 μm.

STRADα knockdown in vivo during corticogenesis results in accumulation of STRADα-deficient cells in the VZ/SVZ. Recently, LKB1 has been implicated in the regulation of neuronal migration during corticogenesis (34). To define the in vivo role of STRADα during neuronal migration, we introduced GFP-shRNA STRADα into E14.0 mouse brains by in utero electroporation (35). GFP-shRNA scram was electroporated in a parallel set of experiments as a control. Sections were stained with Hoechst to visualize cell nuclei and define the zones of the embryonic brain, and the location of GFP$^+$ cells was analyzed at E17.0 and E19.0 (Figure 8). In vivo knockdown of STRADα was confirmed by immunohistochemistry (Figure 9, A and B). At E17.0, GFP-shRNA scram–transfected cells were evenly distributed throughout the developing cortex (Figure 8, A–E). By E19.0, control GFP$^+$ cells were primarily localized in the superficial layers of the CP, in accordance with previous studies (36, 37), and few GFP-shRNA scram–transfected cells were found in the VZ/SVZ and IZ (Figure 8, F–J). STRADα-depleted cells, however, accumulated in the VZ/SVZ at E17.0 and E19.0 (Figure 8, E and J).

To determine whether in vivo knockdown of STRADα induced activation of mTORC1, brain sections from embryos electroporated at E14.0 and sacrificed at E19.0 were probed for P-S6$_{Ser235/236}$ (Figure 9, C and D). GFP$^+$, STRADα-deficient cells exhibited a 42% increase in P-S6 immunoreactivity compared with untransfected neighboring cells and GFP-shRNA scram–transfected controls. Additionally, we evaluated the subcellular localization of LKB1 in electroporated brains, which revealed a 25% increase in nuclear LKB1 in STRADα-depleted GFP$^+$ cells compared with GFP-shRNA scram–transfected cells (Figure 9, E and F). Thus, depletion of STRADα during corticogenesis resulted in accumulation of cells within the proliferative zones of the embryonic mouse brain in association with aberrant nuclear accumulation of LKB1 and activation of mTORC1 signaling. These data suggest a causal relationship between STRADα deficiency and the observed findings of mTORC1 hyperactivation, nuclear LKB1 localization, and neuronal heterotopia in PMSE cortex.

Discussion

We provide the first data to our knowledge in support of a pivotal role for STRADα during cortical development. Our findings in vitro and in vivo model the neuropathologic features of cytomegalic cells and aberrant mTORC1 activation found in PMSE brain tissue. Depletion of STRADα in mNPCs in vitro caused dysregulation of mTORC1 signaling, as evidenced by rapamycin-dependent S6 hyperphosphorylation and cytomegaly. LKB1 was abnormally localized in the nucleus in PMSE neurons and STRADα-deficient mNPCs, which indicates that STRADα depletion disrupts nucleocytoplasmic transport of LKB1 and suggests a possible mechanism for aberrant mTORC1 signaling in STRADα-deficient tissue. Finally, our results suggest a role for STRADα in modulation of cortical lamination, since STRADα knockdown in embryonic brains led to altered lamination that was similar to the neuronal heterotopias present in the PMSE cortex.

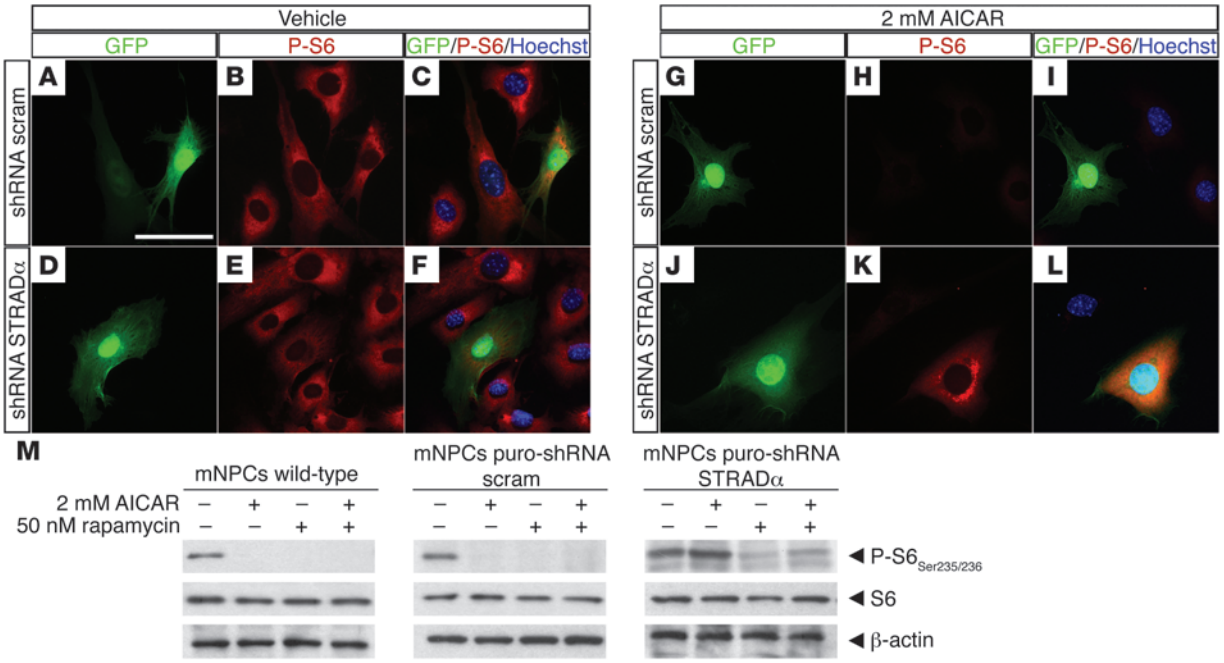

Figure 5

Knockdown of STRADα ameliorates AICAR-mediated inhibition of mTORC1 signaling in a rapamycin-dependent manner. (**A**–**L**) Transient STRADα knockdown led to hyperphosphorylation of S6 after AICAR treatment. mNPCs were transfected with GFP-shRNA scram (**A**–**C** and **G**–**I**) or GFP-shRNA STRADα (**D**–**F** and **J**–**L**), and at 5 DPT were serum starved and treated with either vehicle (**A**–**F**) or 2 mM AICAR (**G**–**L**) for 12 hours. mNPCs were immunostained for P-S6$_{Ser235/236}$. Nuclei were visualized with Hoechst (blue, **C**, **F**, **I**, and **L**). (**M**) Stable STRADα knockdown in mNPCs prevented AICAR-mediated inhibition of S6 phosphorylation in a rapamycin-dependent manner. Wild-type and stably transfected (puro-shRNA scram and puro-shRNA STRADα) mNPCs were serum starved and treated with 2 mM AICAR for 12 hours, 50 nM rapamycin for 1.5 hours, or 2 mM AICAR for 12 hours followed by 50 nM rapamycin for 1.5 hours. Immunoblotting for P-S6$_{Ser235/236}$ revealed that STRADα-depleted mNPCs failed to attenuate P-S6 levels after 2 mM AICAR treatment, in contrast to control cells. Rapamycin treatment attenuated P-S6$_{Ser235/236}$ in STRADα-depleted mNPCs. Immunoblotting for total S6 protein revealed stable S6 expression in all cell types and treatment conditions. Blots were reprobed with β-actin to assess equal loading. Scale bar: 100 μm.

We acknowledge some caveats regarding our results. First, in view of the rarity of PMSE, we had a single postmortem brain specimen for analysis. However, all existing pedigrees have been mapped to the identical *STRADA* gene deletion, and brain MRI reveals evidence of cortical malformation in all PMSE patients. Additionally, the penetrance for epilepsy, cognitive disability, and macrocephaly is 100% in PMSE patients, providing a compelling link between *STRADA* mutations and the neurological phenotype. In the future, high-resolution neuroimaging of PMSE parents would be useful to confirm that heterozygous carriers do not exhibit alterations in brain structure as well. To expand on our findings in PMSE brain tissue, we demonstrated aberrant mTORC1 signaling in immortalized lymphoblasts generated from 3 additional PMSE patients. Second, although nuclear localization of LKB1 and mTORC1 hyperactivation in PMSE neurons suggests one potential pathogenic mechanism for PMSE, there are other possible consequences of STRADα deletion during brain development. Finally, future studies in postnatal animals are needed to determine whether embryonic knockout or knockdown of STRADα is associated with learning deficits or spontaneous seizures.

Regulation of LKB1 activity by STRADα. The abnormal nuclear accumulation of LKB1 in cortical PMSE neurons and STRADα-deficient cells in vitro and in vivo suggests a potential pathogenic mechanism for PMSE. Recently, a role for STRADα in nucleocytoplasmic transport of LKB1 has been defined in non-neuronal cells. STRADα orchestrates nuclear export of LKB1 by serving as an adapter between LKB1 and the nuclear export proteins chromosomal region maintenance 1 (CRM1) and exportin7 and prevents nuclear import of LKB1 by competing with importin-α for LKB1 binding (4). Normal LKB1 function requires cytoplasmic localization of the kinase, since mutations in the LKB1 nuclear localization sequence do not alter LKB1-dependent suppression of cell growth (7). Furthermore, LKB1-SL26 reported in syndromic PJS represents the only known loss-of-function mutation that does not compromise the catalytic activity of LKB1, but instead abolishes its interaction with STRADα (3, 4, 38). Unlike expression of wild-type LKB1, expression of LKB1-SL26 results in exclusively nuclear accumulation of LKB1 in HeLa cells (4). Similarly, the truncated STRADα mutant (residues 1–251) found in PMSE does not bind to LKB1 in vitro, which supports our hypothesis and provides a plausible mechanism to explain nuclear localization of LKB1 in PMSE. Thus, we propose that loss of STRADα in PMSE leads to mTORC1 pathway activation in part by trapping LKB1 in the nucleus. Intrinsic LKB1 catalytic activity is also likely reduced in PMSE, since STRADα binding facilitates LKB1 function (3, 5, 9).

Role of STRADα during corticogenesis. The anomalies in cortical lamination after STRADα knockdown in utero suggest that STRADα plays an important role in assembly of normal hexalaminar cortical architecture. STRADα is expressed throughout the embryonic brain, suggestive of functions in progenitor cells,

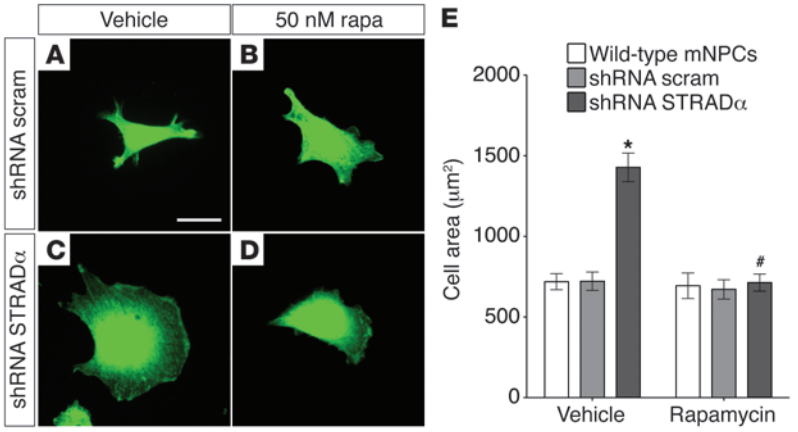

Figure 6

Knockdown of STRADα in mNPCs results in cytomegaly that is prevented by rapamycin treatment. (**A**–**D**) mNPCs were transfected with GFP-shRNA scram (**A** and **B**) or GFP-shRNA STRADα (**C** and **D**) and cultured for 10 days in the absence (**A** and **C**) or presence of daily 50 nM rapamycin treatment (**B** and **D**). In the absence of 50 nM rapamycin, GFP-shRNA STRADα–transfected mNPCs were larger than GFP-shRNA scram–transfected cells. Daily rapamycin treatment prevented STRADα-mediated cytomegaly (**D**). (**E**) Quantification of cell area of untransfected wild-type, GFP-shRNA scram–transfected, and GFP-shRNA STRADα–transfected mNPCs in the absence (vehicle) and presence of daily 50 nM rapamycin treatment. The experiment was conducted 2 separate times. Data are mean ± SEM (n = 30 cells per transfection and treatment condition). $^{*}P < 0.01$ versus other vehicle-treated groups; $^{\#}P < 0.01$ versus vehicle-treated GFP-shRNA STRADα–transfected cells. Scale bar: 20 μm.

as well as in migrating and mature neurons. Targeted STRADα knockdown at E14.0 in vivo led to accumulation of cells in the VZ/SVZ. These findings model the cortical and periventricular malformations in PMSE brains (1) and suggest a causal link between STRADα deficiency and abnormalities of cortical development. Although our quantitative immunohistochemistry revealed a 36% decrease in STRADα expression after in utero knockdown, immunodensitometry provides at best semiquantitative estimation of true protein expression levels. Furthermore, extrapolation of the effects of protein reduction in the rodent to the human brain may not be uniform. The observations of differentially affected cell types, such as heterotopic neurons and cytomegalic cells, in PMSE cortex suggest that loss of STRADα may have distinct effects on progenitor cells in the developing human brain that are mirrored by differential effects of STRADα knockdown on migrating neurons, in which some cells remain trapped in the VZ/SVZ and a few embark on limited migratory pathways.

STRADα expression overlaps with that of LKB1 in the developing brain, and targeted knockdown of LKB1 at E14.0 leads to a similar — although not identical — focal cortical malformation, with migratory arrest of neurons in the IZ of the cortex (34). Furthermore, STRADα-deficient cells exhibit abnormal nuclear localization of LKB1 in vivo, which supports a functional link between STRADα and LKB1 during corticogenesis. LKB1-knockout mice exhibit defects in neural tube closure and are nonviable by E11.0 (39). Knockdown of LKB1 or STRADα in E18 rat hippocampal neurons inhibits axonogenesis, whereas overexpression of either protein results in supernumerary axons (40). Conditional knockout of LKB1 in dorsal telencephalic progenitors (e.g., $Emx^{Cre/+}$ and $Lkb1^{fl/fl}$) in vivo results in reduction of cortical axons through a mechanism dependent on synapses of amphid defective (SAD) protein family members A and B (27, 41). Because loss of LKB1 appears to affect several stages of corticogenesis, further studies are needed to determine whether loss of STRADα causes disturbances in cell cycle regulation, differentiation, or migration.

Although our data demonstrated a critical regulatory role for STRADα on LKB1-mediated mTORC1 signaling during corticogenesis, we find the phenotypic disparities between PMSE and PJS intriguing. To our knowledge, there are no clinical similarities between PMSE and PJS. Why, then, do PMSE patients not develop PJS? One possible explanation may be that STRADα is functionally related to a distinct isoform, STRADβ (2q33.1), that binds and exports LKB1 out of the nucleus and augments catalytic activity of LKB1 — albeit to a lesser extent — toward AMPK-related kinases (5, 6). Unlike STRADα, which is expressed throughout the developing brain, expression of STRADβ is confined to the CP (27). In fact, probing mNPCs along with adult and fetal mouse whole brain lysates for STRADβ expression using 2 different commercially available Abs revealed lack of STRADβ expression in mNPCs (Supplemental Figure 6). The differential cortical expression of STRAD isoforms may account for the inability of STRADβ to compensate for loss of STRADα during the early stages of corticogenesis.

In addition, STRADβ, but not STRADα, is expressed in the gastrointestinal system, which may account for lack of PJS-associated gastrointestinal polyposis in PMSE. On the other hand, neurological features, such as epilepsy or mental retardation, have not to our knowledge been documented in PJS. The striking disparity between PJS and PMSE suggests that STRADα may have some LKB1-independent functions that may be critical for normal brain development. Future studies aimed at identifying alternative binding partners of STRADα may uncover novel pathways that contribute to the neuropathogenesis of PMSE.

mTORC1 hyperactivity and neurocognitive disorders. Our data suggest that STRADα deficiency augments mTORC1 signaling in brain tissue and immortalized lymphocytes from PMSE patients, after STRADα knockdown in mNPCs in vitro, and in the developing cortex in vivo. Aberrant mTORC1 signaling has been implicated in several disorders associated with altered brain architecture, epilepsy, and cognitive disability. Inactivating *TSC1* or *TSC2* mutations cause TSC, an autosomal-dominant disorder characterized by epilepsy, cognitive impairment, and autism (42). Conditional knockout of *Tsc1* or *Tsc2* in the mouse results in enhanced mTORC1 signaling, cytomegaly, altered dendritic spine architecture, poor open field memory task performance, and recurrent seizures (43, 44). Human and mouse neural tissue lacking TSC1 or TSC2 exhibits constitutive mTORC1 activation in association with cytomegaly (43, 45–47). Deletion of *Tsc1* in mouse postnatal forebrain neurons (i.e., $Tsc1^{cc}$–CaMKII-Cre) or knockout of *Tsc2* in radial glia cells (i.e., $Tsc2^{fl/ko}$; hGFAP-Cre) results in severe macrocephaly secondary to cellular hypertrophy (46, 47). Mutations in *PTEN* have been reported in patients with autism and concomitant macrocephaly, and conditional deletion of *PTEN* in differentiated neurons in vivo leads to mac-

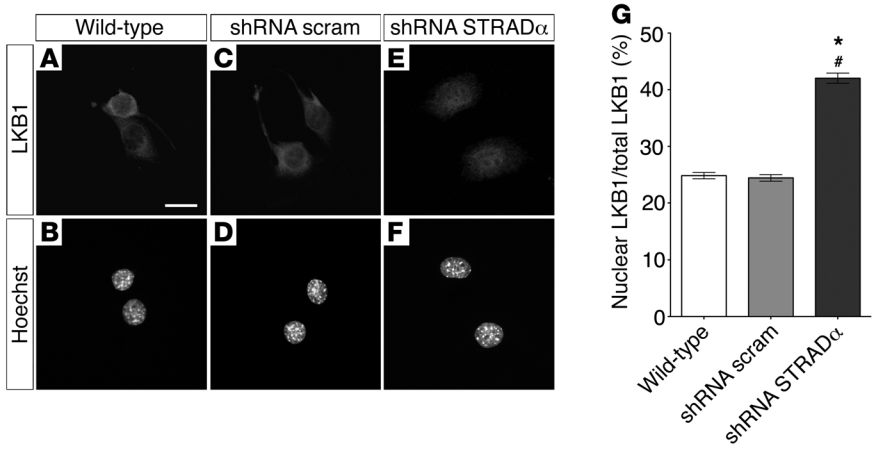

Figure 7
STRADα depletion in mNPCs causes nuclear accumulation of LKB1. (**A**–**F**) Wild-type mNPCs (**A** and **B**) and mNPCs stably transfected with puro-shRNA scram (**C** and **D**) and puro-shRNA STRADα (**E** and **F**) were immunostained for LKB1 (**A**, **C**, and **E**). Nuclei were visualized with Hoechst staining (**B**, **D**, and **F**). The STRADα-depleted mNPCs exhibited increased nuclear LKB1 localization compared with wild-type and puro-shRNA scram–transfected mNPCs. (**G**) Quantification of nuclear LKB1 localization. STRADα-depleted cells had 69% more nuclear LKB1 (n = 149; 42%) than did wild-type cells (n = 132; 25%) and 73% more than did puro-shRNA scram–transfected cells (n = 143; 24%). Data (mean ± SEM) show nuclear LKB1 as a percentage of total LKB1. *P < 0.01 versus wild-type; #P < 0.01 versus puro-shRNA scram. Scale bar: 20 μm.

rocephaly, neuronal hypertrophy, and abnormal social behaviors in association with aberrant mTORC1 signaling (22, 23, 48).

Rapamycin, a specific inhibitor of mTOR, has been used successfully in these models to prevent or rescue mTORC1-dependent neuronal phenotypes. For example, rapamycin application prevents neuronal cytomegaly and restores dendritic spine morphology following *Tsc2* knockdown (43). Moreover, rapamycin treatment normalized the threshold for late-phase long-term potentiation induction in *Tsc2*$^{+/-}$ mice and notably prevented the onset of learning deficits in multiple learning paradigms in this strain (46). A direct link between epileptogenesis and mTORC1 signaling has recently been demonstrated: temporal lobe seizures induced by acute kainate application in rats resulted in hyperphosphorylation of S6, and pretreatment with rapamycin before seizure induction led to a reduction in hippocampal mossy fiber sprouting and neuronal death (49). We showed here that rapamycin prevented cytomegaly and mTORC1 activation caused by STRADα deficiency in mNPCs. Our results add *STRADA* to the growing repertoire of genes whose mutations lead to aberrant mTORC1 activation and neurodevelopmental disorders associated with epilepsy, altered brain structure, and cognitive disability. As several human trials underscore the therapeutic potential of rapamycin and other mTOR inhibitors in the treatment of mTORC1-associated disorders such as TSC (50, 51), early treatment with mTOR inhibitors may prevent the devastating neurological features of PMSE.

Methods

All animal experiments were approved by the Institutional Animal Care and Use Committee of the University of Pennsylvania. All human studies were approved by the Institutional Review Board of Lancaster General Hospital (Lancaster, Pennsylvania, USA). Parents provided informed consent prior to their own and their children's participation.

Human brain specimens. Sporadic type I and type II focal cortical dysplasia specimens were obtained from 8 patients (mean age, 5.1 years; 60% male) who underwent epilepsy surgery (Academic Medical Center, University of Amsterdam, Netherlands; Children's Hospital of Philadelphia, Philadelphia, Pennsylvania, USA; and National Hospital for Neurology and Neurosurgery, London, United Kingdom). 1 postmortem PMSE brain (7-month-old female) was procured from the Clinic for Special Children (Lancaster, Pennsylvania, USA). Cortical dysplasia focal epilepsy syndrome specimens (n = 3; mean age, 4 years; 66% male) were obtained following surgical resection for epilepsy treatment (Children's Hospital of Philadelphia; ref. 26). Cortical dysplasia focal epilepsy syndrome specimens were used as an epilepsy control in immunohistochemical experiments unless otherwise indicated. Hemimegalencephaly specimens (n = 2; mean age, 7.5 months; 100% female) were obtained following surgical resection for epilepsy treatment (Academic Medical Center, University of Amsterdam, Netherlands). Cortical tubers were obtained from TSC patients (n = 8; mean age, 7.2 years; 50% male) with TSC defined by clinical criteria. Nonepilepsy control cortical specimens were obtained from 2 temporal, 2 frontal, and 2 parietal regions at necropsy from 6 patients (mean age, 5.8 years; 50% male) who died of non-neurologic causes (Brain and Tissue Bank for Developmental Disorders, University of Maryland, College Park, Maryland, USA; and Children's Hospital of Philadelphia). All specimens were fixed in 4% paraformaldehyde, embedded in paraffin, and cut into 7-μm sections.

Immunohistochemistry. Paraffin-embedded, formalin-fixed human brain sections were immersed in a solution containing 150 ml methanol and 30 ml H_2O_2 (30%) for 30 minutes. Sections were blocked in a solution containing 2% FBS and 0.1M Tris for 5 minutes. Primary Ab labeling was performed overnight at 4°C. When necessary, antigen unmasking was performed using Antigen Unmasking Solution (Vector Labs) according to the manufacturer's protocol. Biotinylated secondary Abs (diluted 1:1,000; Vector Labs) were applied for 1 hour at room temperature. Ab binding was detected by incubation with the avidin-biotin complex (Vectastain ABC Kit; Vector Labs) and developed with 3,3′-diaminobenzidine (Sigma-Aldrich). Sections were counterstained with LFB-CV using standard protocols and imaged using a Leica DM4000 B microscope attached to a Leica DC 480 camera. The following primary Abs were used: rabbit polyclonal Ab (pAb) to STRADα (diluted 1:100; Abcam); rabbit mAb to LKB1 (diluted 1:100; Cell Signaling); rabbit pAb to LKB1 (diluted 1:100; Novus Biologicals); rabbit pAb to LKB1 (diluted 1:100; Santa Cruz); rabbit mAb to P-S6K$_{Thr389}$ (diluted 1:100; Novus Biologicals); rabbit pAb to P-S6$_{Ser235/236}$ (diluted 1:50; Bethyl Laboratories); mouse mAb to c-Myc (diluted 1:500, Abcam), and mouse mAb to NeuN (diluted 1:500, Millipore). The anti-STRADα Ab recognizes amino acids 31–66 that are excluded from the human deletion, and thus would detect STRADα if a truncated isoform was expressed. To determine the number of cells in human brain samples that exhibit predominately nuclear LKB1 immunostaining (nuclear/cytoplasmic LKB1 expression ratio greater than 1), hand counts were performed on LKB1-stained sections that were imaged using a ×40 objective.

Mouse brains were fixed in 4% PFA, cryoprotected in a sucrose gradient, and frozen in OCT (Tissue Tek) on an isopropanol/dry ice mixture. Coronal sections (20 μm) were cut with a cryostat. Sections were permea-

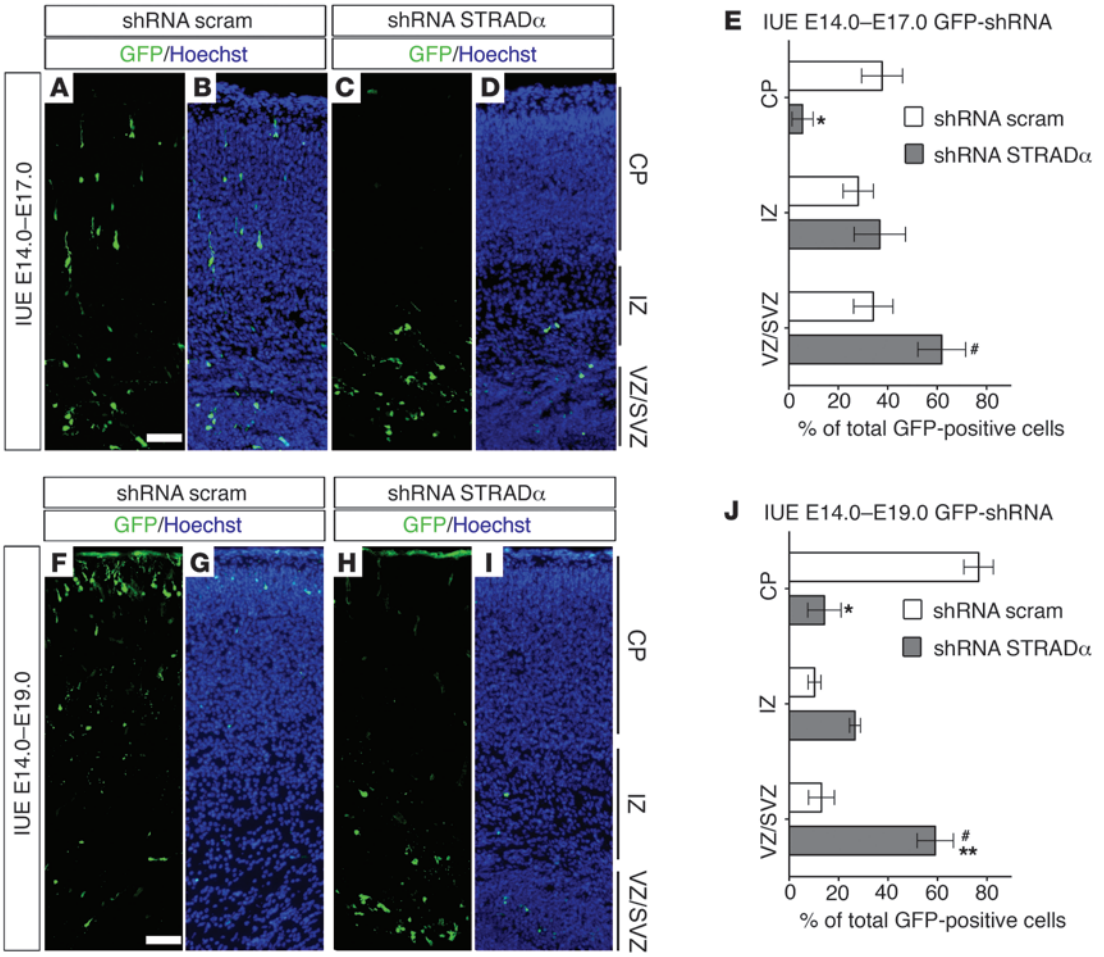

Figure 8

Knockdown of STRADα in vivo leads to aberrant cortical lamination. In utero electroporation (IUE) was performed at E14.0 using GFP-shRNA scram (**A**, **B**, **F**, and **G**) or GFP-shRNA STRADα (**C**, **D**, **H**, and **I**). Localization of transfected cells in the embryonic mouse brain was analyzed at E17.0 (**A**–**D**) and E19.0 (**F**–**I**). Nuclei were visualized with Hoechst staining (blue, **B**, **D**, **G**, and **I**). At E17.0, control GFP-shRNA scram–transfected cells were evenly distributed among the CP (38% ± 8%), IZ (28% ± 6%), and VZ/SVZ (34% ± 8%). By E19.0, the majority of GFP-shRNA scram–transfected cells reached the superficial layers of the CP (77% ± 6%). STRADα-depleted cells, however, accumulated in the VZ/SVZ at E17.0 (**C** and **D**; 62% ± 10%) and E19.0 (**H** and **I**; 59% ± 7%). (**E** and **J**) Percent transfected GFP$^+$ cells in each zone of the developing brain at E17.0 (**E**) and E19.0 (**J**). Data are mean ± SEM ($n = 5$). *$P < 0.05$ versus CP GFP-shRNA scram; **$P < 0.05$ versus VZ/SVZ GFP-shRNA scram; $^{\#}P < 0.05$ versus CP GFP-shRNA STRADα. Scale bars: 50 μm.

bilized with 0.3% Triton and blocked for 1.5 hours in 5% normal serum from the species in which the secondary Ab was raised. When 2 different secondary Abs were used, sections were blocked in 2.5% serum from each host. Primary Abs were diluted in 5% serum and applied overnight at 4°C. Secondary Abs were added for 1.5 hours at room temperature, and sections were counterstained with Hoechst 33342 (0.0001 μg/μl; Invitrogen) for 20 minutes and coverslipped in mounting media (Fluoromount-G; SouthernBiotech). The following primary Abs were used: rabbit pAb to STRADα (diluted 1:100; Abcam); mouse mAb to MAP2 (diluted 1:500; Abcam); and mouse mAb to nestin (diluted 1:100; Millipore). The following secondary Abs were used: Texas Red anti-rabbit (diluted 1:100; Vector Labs); Texas Red anti-mouse (diluted 1:100; Vector Labs); Fluorescein anti-rabbit (diluted 1:100; Vector Labs). Images were acquired using a Leica DM4000 B microscope with a DFC340 FX camera using EL 6000 fluorescent source, followed by analysis with Image-Pro Plus (Media Cybernetics) or a Leica TCS 4D laser scanning confocal microscope and image processing using Adobe Photoshop.

Culture and transfection. mNPCs (provided by J. Wolfe, Children's Hospital of Philadelphia; ref. 28) were cultured on poly-D-lysine–coated plates (10 μg/ml; Sigma-Aldrich) in DMEM/F12 (Invitrogen) supplemented with 1% N_2 (Invitrogen), 1% FBS (Sigma-Aldrich), 1% penicillin/streptomycin (Invitrogen), 20 ng/ml basic fibroblast growth factor (Promega), and heparin (5 μg/ml; Sigma-Aldrich). mNPCs were transfected with 1 μg plasmid diluted in 100 μl Opti-MEM (Invitrogen) using Lipofectamine LTX and PLUS Reagent (Invitrogen) according to the manufacturer's protocol. The following plasmids were purchased from SABiosciences: KM41633G (GFP-shRNA STRADα and GFP-shRNA scram) and KM41633P (puro-shRNA STRADα and puro-shRNA scram). Prior to transfection, plasmids were amplified by transformation of Subcloning Efficiency DH5α Chemically Competent *E. coli* (Invitrogen) and purified using EndoFree Plasmid Maxi Kit (Qiagen). At 5 DPT, the GFP$^+$ mNPCs were sorted using a BD FACSVantage SE flow cytometer (BD Biosciences) available at the Penn Flow Cytometry and Cell Sorting Facility. 3 experimental replicates were done. For stable transfection, cells were cultured in the presence of 6 μg/ml puromycin (Invitrogen) beginning

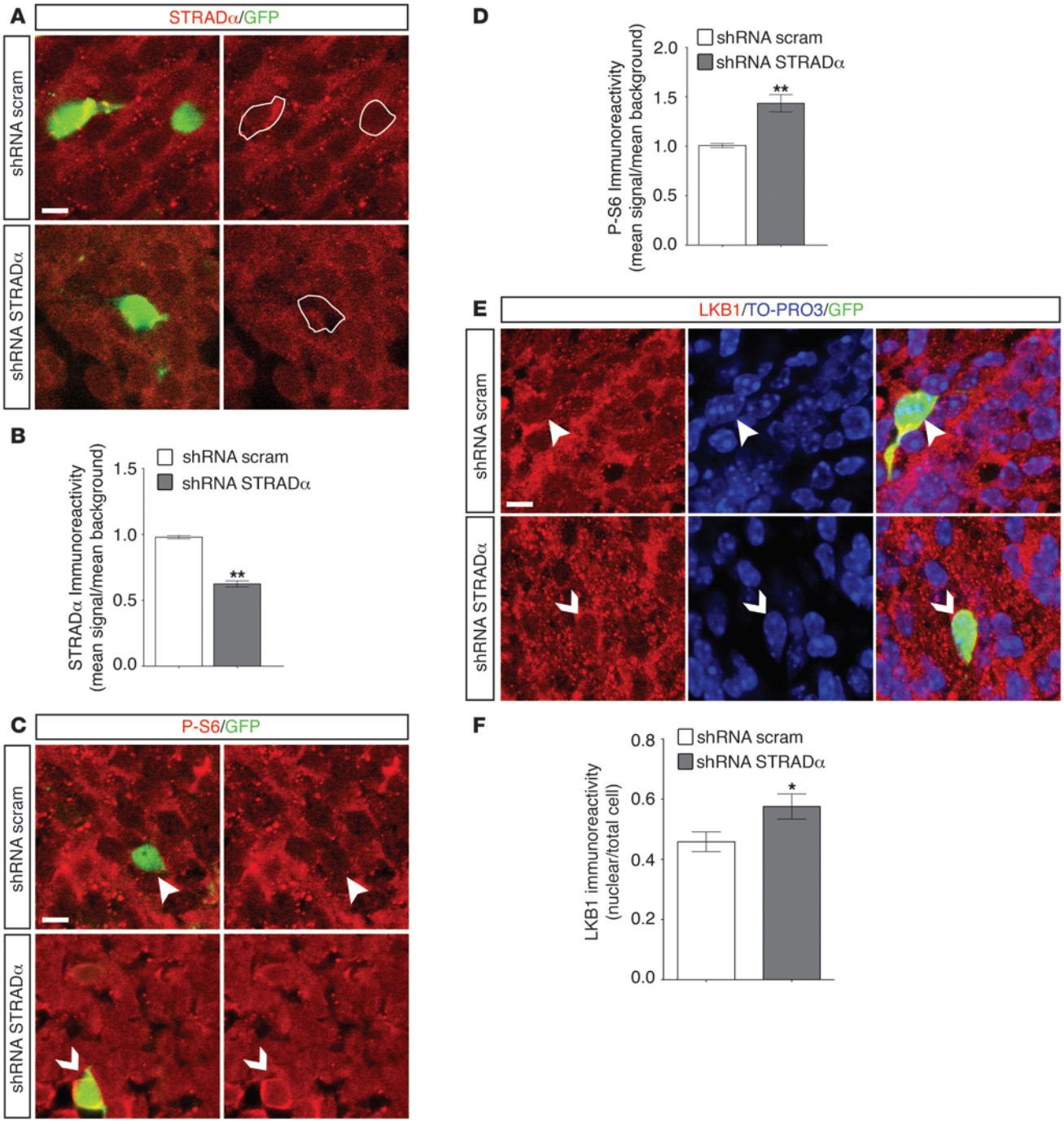

Figure 9

STRADα-deficient cells exhibit enhanced phosphorylation of S6 and nuclear LKB1 localization in vivo. In utero electroporation was performed at E14.0 with GFP-shRNA STRADα and GFP-shRNA scram, and brains were analyzed at E19.0 by immunostaining for STRADα (**A** and **B**), P-S6$_{Ser235/236}$ (**C** and **D**), and LKB1 (**E** and **F**). (**A** and **B**) GFP-shRNA STRADα–transfected cells expressed less STRADα than did GFP-shRNA scram–transfected and untransfected cells. White outlines represent the location of the GFP$^+$ cells. Quantification revealed a 36% decrease in STRADα immunoreactivity. (**C** and **D**) GFP-shRNA STRADα–transfected cells exhibited enhanced P-S6 immunoreactivity compared with untransfected cells and GFP-shRNA scram–transfected cells. Arrowheads denote GFP$^+$ cells. Quantification revealed a 42% increase in P-S6 levels. (**E** and **F**) GFP-shRNA STRADα–transfected cells exhibited enhanced nuclear LKB1 compared with GFP-shRNA scram–transfected cells. Nuclei were visualized with TO-PRO3. Arrowheads denote GFP$^+$ cells. Quantification revealed a 25% increase in nuclear/total LKB1 in STRADα-depleted cells. Data (mean ± SEM) are mean signal/background (**B** and **D**) or mean nuclear/total LKB1 (**F**) (n = 10). *P < 0.05; **P < 0.01. Scale bars: 6.08 μm.

48 hours post transfection. Colonies were obtained by placing single transfected cells into each well of a poly-D-lysine–coated plate. Knockdown was assessed by Western blotting 3 separate times. Cultures were maintained at 37°C in humidified 5% CO_2 incubators. For drug treatment experiments, mNPCs were serum starved by replacing complete medium with DMEM/F12 for 12 hours. AICAR (2 mM; Cell Signaling) and rapamycin (50 nM; Cell Signaling) were added directly to cells for 12 and 1.5 hours, respectively. For cell size studies, 50 nM rapamycin was added daily. Wild-type and LKB1-null MEFs were a gift from the laboratories of L. Cantley (Beth Israel Deaconess Medical Center, Boston, Massachusetts, USA) and R. Shaw (Salk Institute for Biological Sciences, La Jolla, California, USA) (8, 13). MEFs were cultured in DMEM (Invitrogen) supplemented with 10% FBS (Sigma-Aldrich) and 1% penicillin/streptomycin (Invitrogen). MEFs were serum starved overnight with or without AICAR treatment (2 mM; Cell Signaling), followed by treatment with rapamycin (50 nM; Cell Signaling). To establish LCLs, peripheral blood from PMSE patients (n = 3), heterozygous parents (n = 4), and controls (n = 2) was obtained from the Clinic for Special Children. Peripheral blood mononuclear cells were collected following a Ficoll gradient (GE Healthcare) and transformed by infection with Epstein-Barr virus according to established protocol, with the help of M. Deardorff's laboratory (Children's Hospital of Philadelphia). LCLs were grown in RPMI 1640 (Invitrogen) with 20% FBS (Sigma-Aldrich), 0.5% penicillin/streptomycin, and 2% L-glutamine (Invitrogen). For drug treatments, LCLs were serum starved for 12 hours and pretreated with 5 μM STO-609 (Tocris Biosciences) for 1 hour, followed by treatment with 10 μM oligomycin (Sigma-Aldrich) for 3 hours.

Western blotting. Cells were lysed on ice for 20 minutes in RIPA lysis buffer (50 mM Tris HCl, pH 8.0; 150 mM NaCl; 1% NP-40; 0.5% sodium deoxycholate; and 0.1% SDS) with protease (Sigma-Aldrich) and phosphatase inhibitor mixtures (Thermo Fisher Scientific). Lysates were centrifuged at 4°C for 20 minutes at 12,000 *g*, and the supernatants were collected. Protein concentrations were determined using the DC Protein Assay Kit (Bio-Rad), and equal amounts of total protein (20–40 μg) were combined with 4× reducing sample loading buffer and denatured at 95°C for 5 minutes. The samples were subjected to electrophoresis on a 4%–15% SDS-PAGE (Bio-Rad) and transferred onto PVDF membranes at 4°C. The membranes were blocked in TBS, 0.1% Tween 20, plus 5% nonfat dry milk for 1 hour. Membranes were probed overnight at 4°C with the following primary Abs: rabbit pAb to STRADα (diluted 1:100; Abcam), rabbit mAb to P-$S6_{Ser235/236}$ (diluted 1:2,000; Cell Signaling), rabbit mAb to S6 (diluted 1:1,000; Cell Signaling), rabbit pAb to SOX2 (diluted 1:1,000; Abcam), rabbit pAb to P-ACC_{Ser79} (diluted 1:1,000; Cell Signaling), or rabbit pAb to STRADβ (diluted 1:1,000; Anaspec; diluted 1:10,000; Abcam). Membranes were incubated with HRP-conjugated secondary Abs (diluted 1:3,000; GE Healthcare) for 1 hour at room temperature. The ECL detection system (GE Healthcare) was used prior to exposure of membranes to X-ray film (Kodak). To ensure equal loading, membranes were stripped in Restore Western Blot Stripping Buffer (Thermo Fisher Scientific); blocked; subjected to Western blot analysis as described above; and probed as follows: rabbit mAb to GAPDH (diluted 1:4,000; Cell Signaling) followed by HRP-conjugated anti-rabbit (diluted 1:3,000; GE Healthcare) or mouse mAb to HRP–β-actin (diluted 1:5,000; Abcam).

Immunocytochemistry. mNPCs were fixed in 4% PFA at room temperature for 15 minutes, permeabilized in PBS plus 0.3% Triton X-100, and blocked for 2 hours in 5% normal serum from the species in which the secondary Ab was raised. Cells were incubated in primary Abs in 5% normal serum at 4°C overnight and then in fluorochrome-conjugated secondary Abs for 2 hours at room temperature. The following primary Abs were used: rabbit pAb to STRADα (diluted 1:100; Abcam); rabbit mAb to P-$S6_{Ser235/236}$ (diluted 1:200; Cell Signaling); rabbit pAb to LKB1 (diluted 1:100; Santa Cruz); and rabbit pAb nestin (diluted 1:500; Abcam). The following secondary Abs were used: Texas Red anti-rabbit (diluted 1:100; Vector Labs) and Fluorescein anti-rabbit (diluted 1:100; Vector Labs). Cells were incubated in Hoechst 33342 (0.0001 μg/μl, Invitrogen) for 20 minutes and mounted onto slides using Fluoromount-G (SouthernBiotech). Images were obtained using a Leica DM4000 B microscope with a DFC340 FX camera using EL 6000 fluorescent source. Image Pro-Plus 6.2 software and Adobe Photoshop were used for image processing.

In utero electroporation. Timed pregnant females (E14.0) were placed under isoflurane-induced anesthesia, and the uterine horns were surgically exteriorized. Plasmid DNA (5 μg/μl) diluted in Fast Green dye (0.3 mg/ml; Sigma-Aldrich) was microinjected through the uterine wall into one of the lateral ventricles of the embryos. 5 electrical pulses (40 V, 50-ms duration, at 1,000-ms intervals; ref. 35) were delivered across the uterine wall and the embryonic head using CUY21Edit Square Wave Electroporator (Nepagene). The uterine horns were then returned into the pelvic cavity, and the abdominal wall and skin were sutured. The pregnant dam was returned to the animal colony. Embryos were sacrificed at E17.0 and E19.0.

Quantitative analysis. For measurement of cell area, images were processed by Image Pro Plus (Media Cybernetics). Total cell area was quantified by outlining the periphery of the GFP^+ cells and then applying the area measurement function. Untransfected cells were identified by immunostaining for nestin (Rabbit pAb to nestin, diluted 1:500; Abcam) followed by Texas Red anti-rabbit (diluted 1:100; Vector Labs). Nestin staining was enhanced by using contrast enhancement in order to clearly delineate the cell boundaries (n = 30 cells per condition per drug treatment).

To quantify subcellular LKB1 localization, LKB1 immunofluorescence was measured in the whole cell as well as in the Hoechst-stained nuclear area using the Histogram function. Total mean nuclear intensity was divided by total mean cellular intensity to yield percent nuclear LKB1 localization.

For the location of shRNA-transfected cells in vivo, in utero electroporation was performed, targeting the same area of the cortex of 5 animals for each plasmid and each time point. At E17.0 and E19.0, fixed frozen sections were counterstained with Hoechst (0.0001 μg/μl; Invitrogen). Images were acquired using a Leica DM4000 B microscope with a DFC340 FX camera and subsequently processed using Image Pro Plus (Media Cybernetics). The 3 zones of the developing embryonic brain (VZ/SVZ, IZ, and CP) were identified by the distinguishing density of Hoechst-positive nuclei. The region of interest (ROI) was delineated by a rectangle that extended from the pial surface to the lateral ventricles. The number of GFP^+ cells within each zone, as well as the total number of GFP^+ cells in the ROI, was counted using the software and verified by a hand count. A total of 4 sections from each of the 5 animals per time point and plasmid was analyzed.

To quantify fluorescence intensity in electroporated brains at E19.0, brain sections were immunostained with rabbit pAb to STRADα (diluted 1:100; Abcam), rabbit mAb to P-$S6_{Ser235/236}$ (diluted 1:200; Cell Signaling), or rabbit pAb to LKB1 (diluted 1:100; Novus) and counterstained with either Hoechst 33342 (0.0001 μg/μl; Invitrogen) or To-Pro3 (diluted 1:10,000; Invitrogen). Images were acquired using a laser-scanning confocal microscope (TCS 4D; Leica) and processed using Image Pro Plus (Media Cybernetics). To calculate immunoreactivity of STRADα and P-S6, the GFP^+ cells were outlined using the ROI function, and subsequently, the same ROI was placed at the location of the GFP^+ cell on the channel containing the immunolabeled image. The fluorescence intensity of each Ab was measured using the Histogram function. All fluorescent intensities were normalized to the intensities of neighboring untransfected cells (n = 10 cells per transfection condition). For the subcellular localization of LKB1, the intensity of LKB1 immunoreactivity was measured using the Histogram function of the entire GFP^+ cell as well as the nucleus, as defined by To-Pro3 staining (n = 10 cells per transfection condition).

Statistics. Data are mean ± SEM. Prism software (Prism 5) was used for statistical analysis. In all comparisons, a P value less than 0.05 was con-

sidered significant. Cell area measurements represent mean cell area; 1-way ANOVA followed by Turkey-Kramer post hoc analysis for multiple comparisons were computed to determine significance. Subcellular LKB1 localization is reported as percent mean nuclear intensity; unpaired 2-tailed Student's *t* test was computed to determine significance. In vivo shRNA-transfected cell location data represent percent GFP^+ cells in each zone relative to the total GFP^+ cells in a given ROI; significance was determined by 1-way ANOVA followed by Dunnett post-hoc analysis for multiple comparisons, in accordance with previously published methodology (52). STRADα and P-S6 immunoreactivity measurements represent mean signal/background, and LKB1 immunoreactivity values represent mean nuclear relative to total cellular LKB1 intensity; statistical significance was calculated by unpaired 2-tailed Student's *t* test.

Acknowledgments

This work was supported by NIH grant NS045877 (to P.B. Crino). The authors thank M. Deardorff for help with establishment of LCLs, R. Wilensky for microscope use, and S. Scherer for critical review of this manuscript.

Received for publication October 28, 2009, and accepted in revised form January 28, 2010.

Address correspondence to: Peter B. Crino, Department of Neurology, University of Pennsylvania, 3 West Gates Bldg., 3400 Spruce St., Philadelphia, Pennsylvania 19104, USA. Phone: 215.349.5312; Fax: 215.573.2029; E-mail: peter.crino@uphs.upenn.edu.

1. Puffenberger EG, et al. Polyhydramnios, megalencephaly and symptomatic epilepsy caused by a homozygous 7-kilobase deletion in LYK5. *Brain*. 2007;130(Pt 7):1929–1941.
2. Zeqiraj E, et al. ATP and MO25alpha regulate the conformational state of the STRADalpha pseudokinase and activation of the LKB1 tumour suppressor. *PLoS Biol*. 2009;7(6):e1000126.
3. Baas AF, et al. Activation of the tumour suppressor kinase LKB1 by the STE20-like pseudokinase STRAD. *EMBO J*. 2003;22(12):3062–3072.
4. Dorfman J, Macara IG. STRADalpha regulates LKB1 localization by blocking access to importin-alpha, and by association with Crm1 and exportin-7. *Mol Biol Cell*. 2008;19(4):1614–1626.
5. Boudeau J, et al. MO25alpha/beta interact with STRADalpha/beta enhancing their ability to bind, activate and localize LKB1 in the cytoplasm. *EMBO J*. 2003;22(19):5102–5114.
6. Hawley SA, et al. Complexes between the LKB1 tumor suppressor, STRAD alpha/beta and MO25 alpha/beta are upstream kinases in the AMP-activated protein kinase cascade. *J Biol*. 2003;2(4):28.
7. Tiainen M, Vaahtomeri K, Ylikorkala A, Makela TP. Growth arrest by the LKB1 tumor suppressor: induction of p21(WAF1/CIP1). *Hum Mol Genet*. 2002;11(13):1497–1504.
8. Shaw RJ, et al. The tumor suppressor LKB1 kinase directly activates AMP-activated kinase and regulates apoptosis in response to energy stress. *Proc Natl Acad Sci U S A*. 2004;101(10):3329–3335.
9. Baas AF, et al. Complete polarization of single intestinal epithelial cells upon activation of LKB1 by STRAD. *Cell*. 2004;116(3):457–466.
10. Lizcano JM, et al. LKB1 is a master kinase that activates 13 kinases of the AMPK subfamily, including MARK/PAR-1. *EMBO J*. 2004;23(4):833–843.
11. Zeqiraj E, Filippi BM, Deak M, Alessi DR, van Aalten DM. Structure of the LKB1-STRAD-MO25 complex reveals an allosteric mechanism of kinase activation. *Science*. 2009;326(5960):1707–1711.
12. Corradetti MN, Inoki K, Bardeesy N, DePinho RA, Guan KL. Regulation of the TSC pathway by LKB1: evidence of a molecular link between tuberous sclerosis complex and Peutz-Jeghers syndrome. *Genes Dev*. 2004;18(13):1533–1538.
13. Shaw RJ, et al. The LKB1 tumor suppressor negatively regulates mTOR signaling. *Cancer Cell*. 2004;6(1):91–99.
14. Inoki K, Zhu T, Guan KL. TSC2 mediates cellular energy response to control cell growth and survival. *Cell*. 2003;115(5):577–590.
15. Inoki K, Li Y, Xu T, Guan KL. Rheb GTPase is a direct target of TSC2 GAP activity and regulates mTOR signaling. *Genes Dev*. 2003;17(15):1829–1834.
16. Wullschleger S, Loewith R, Hall MN. TOR signaling in growth and metabolism. *Cell*. 2006;124(3):471–484.
17. Jenne DE, et al. Peutz-Jeghers syndrome is caused by mutations in a novel serine threonine kinase. *Nat Genet*. 1998;18(1):38–43.
18. Jishage K, et al. Role of Lkb1, the causative gene of Peutz-Jegher's syndrome, in embryogenesis and polyposis. *Proc Natl Acad Sci U S A*. 2002;99(13):8903–8908.
19. Bardeesy N, et al. Loss of the Lkb1 tumour suppressor provokes intestinal polyposis but resistance to transformation. *Nature*. 2002;419(6903):162–167.
20. Shackelford DB, et al. mTOR and HIF-1alpha-mediated tumor metabolism in an LKB1 mouse model of Peutz-Jeghers syndrome. *Proc Natl Acad Sci U S A*. 2009;106(27):11137–11142.
21. Maehama T, Dixon JE. The tumor suppressor, PTEN/MMAC1, dephosphorylates the lipid second messenger, phosphatidylinositol 3,4,5-trisphosphate. *J Biol Chem*. 1998;273(22):13375–13378.
22. Waite KA, Eng C. Protean PTEN: form and function. *Am J Hum Genet*. 2002;70(4):829–844.
23. Butler MG, et al. Subset of individuals with autism spectrum disorders and extreme macrocephaly associated with germline PTEN tumour suppressor gene mutations. *J Med Genet*. 2005;42(4):318–321.
24. Roux PP, et al. RAS/ERK signaling promotes site-specific ribosomal protein S6 phosphorylation via RSK and stimulates cap-dependent translation. *J Biol Chem*. 2007;282(19):14056–14064.
25. West MJ, Stoneley M, Willis AE. Translational induction of the c-myc oncogene via activation of the FRAP/TOR signalling pathway. *Oncogene*. 1998;17(6):769–780.
26. Strauss KA, et al. Recessive symptomatic focal epilepsy and mutant contactin-associated protein-like 2. *N Engl J Med*. 2006;354(13):1370–1377.
27. Barnes AP, et al. LKB1 and SAD kinases define a pathway required for the polarization of cortical neurons. *Cell*. 2007;129(3):549–563.
28. Magnitsky S, Walton RM, Wolfe JH, Poptani H. Magnetic resonance imaging detects differences in migration between primary and immortalized neural stem cells. *Acad Radiol*. 2008;15(10):1269–1281.
29. Watson DJ, Walton RM, Magnitsky SG, Bulte JW, Poptani H, Wolfe JH. Structure-specific patterns of neural stem cell engraftment after transplantation in the adult mouse brain. *Hum Gene Ther*. 2006;17(7):693–704.
30. Hardie DG, Scott JW, Pan DA, Hudson ER. Management of cellular energy by the AMP-activated protein kinase system. *FEBS Lett*. 2003;546(1):113–120.
31. Lopez JM, Santidrian AF, Campas C, Gil J. 5-Aminoimidazole-4-carboxamide riboside induces apoptosis in Jurkat cells, but the AMP-activated protein kinase is not involved. *Biochem J*. 2003; 370(Pt 3):1027–1032.
32. Tamas P, et al. Regulation of the energy sensor AMP-activated protein kinase by antigen receptor and Ca2+ in T lymphocytes. *J Exp Med*. 2006;203(7):1665–1670.
33. Lee CH, Inoki K, Guan KL. mTOR pathway as a target in tissue hypertrophy. *Annu Rev Pharmacol Toxicol*. 2007;47:443–467.
34. Asada N, Sanada K, Fukada Y. LKB1 regulates neuronal migration and neuronal differentiation in the developing neocortex through centrosomal positioning. *J Neurosci*. 2007;27(43):11769–11775.
35. Saito T. In vivo electroporation in the embryonic mouse central nervous system. *Nat Protoc*. 2006;1(3):1552–1558.
36. Hack I, et al. Divergent roles of ApoER2 and Vldlr in the migration of cortical neurons. *Development*. 2007;134(21):3883–3891.
37. Molyneaux BJ, Arlotta P, Menezes JR, Macklis JD. Neuronal subtype specification in the cerebral cortex. *Nat Rev Neurosci*. 2007;8(6):427–437.
38. Nezu J, Oku A, Shimane M. Loss of cytoplasmic retention ability of mutant LKB1 found in Peutz-Jeghers syndrome patients. *Biochem Biophys Res Commun*. 1999;261(3):750–755.
39. Ylikorkala A, et al. Vascular abnormalities and deregulation of VEGF in Lkb1-deficient mice. *Science*. 2001;293(5533):1323–1326.
40. Shelly M, Cancedda L, Heilshorn S, Sumbre G, Poo MM. LKB1/STRAD promotes axon initiation during neuronal polarization. *Cell*. 2007;129(3):565–577.
41. Kishi M, Pan YA, Crump JG, Sanes JR. Mammalian SAD kinases are required for neuronal polarization. *Science*. 2005;307(5711):929–932.
42. Crino PB, Nathanson KL, Henske EP. The tuberous sclerosis complex. *N Engl J Med*. 2006;355(13):1345–1356.
43. Tavazoie SF, Alvarez VA, Ridenour DA, Kwiatkowski DJ, Sabatini BL. Regulation of neuronal morphology and function by the tumor suppressors Tsc1 and Tsc2. *Nat Neurosci*. 2005;8(12):1727–1734.
44. Meikle L, et al. A mouse model of tuberous sclerosis: neuronal loss of Tsc1 causes dysplastic and ectopic neurons, reduced myelination, seizure activity, and limited survival. *J Neurosci*. 2007;27(21):5546–5558.
45. Baybis M, et al. mTOR cascade activation distinguishes tubers from focal cortical dysplasia. *Ann Neurol*. 2004;56(4):478–487.
46. Ehninger D, et al. Reversal of learning deficits in a Tsc2+/– mouse model of tuberous sclerosis. *Nat Med*. 2008;14(8):843–848.
47. Way SW, et al. Loss of Tsc2 in radial glia models the brain pathology of tuberous sclerosis complex in the mouse. *Hum Mol Genet*. 2009;18(7):1252–1265.
48. Kwon CH, et al. Pten regulates neuronal arborization and social interaction in mice. *Neuron*. 2006;50(3):377–388.
49. Zeng LH, Rensing NR, Wong M. The mammalian target of rapamycin signaling pathway mediates epileptogenesis in a model of temporal lobe epilepsy. *J Neurosci*. 2009;29(21):6964–6972.
50. Franz DN, et al. Rapamycin causes regression of astrocytomas in tuberous sclerosis complex. *Ann Neurol*. 2006;59(3):490–498.
51. Marsh DJ, et al. Rapamycin treatment for a child with germline PTEN mutation. *Nat Clin Pract Oncol*. 2008;5(6):357–361.
52. Nguyen L, et al. p27kip1 independently promotes neuronal differentiation and migration in the cerebral cortex. *Genes Dev*. 2006;20(11):1511–1524.